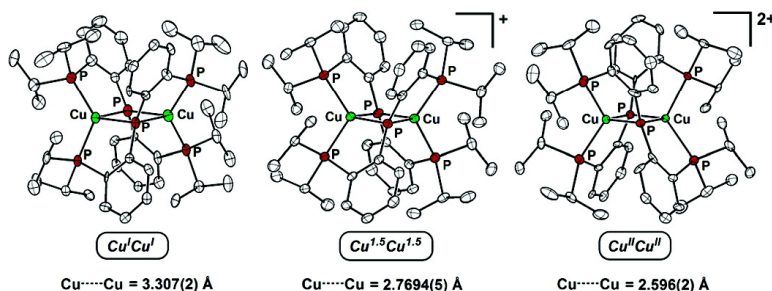


## Structural Snapshots of a Flexible CuP Core that Accommodates the Oxidation States CuCu, CuCu, and CuCu

Neal P. Mankad, Eric Rivard, Seth B. Harkins, and Jonas C. Peters

*J. Am. Chem. Soc.*, **2005**, 127 (46), 16032-16033 • DOI: 10.1021/ja056071I • Publication Date (Web): 28 October 2005

Downloaded from <http://pubs.acs.org> on March 25, 2009



### More About This Article

Additional resources and features associated with this article are available within the HTML version:

- Supporting Information
- Links to the 6 articles that cite this article, as of the time of this article download
- Access to high resolution figures
- Links to articles and content related to this article
- Copyright permission to reproduce figures and/or text from this article

[View the Full Text HTML](#)

## Structural Snapshots of a Flexible $\text{Cu}_2\text{P}_2$ Core that Accommodates the Oxidation States $\text{Cu}^I\text{Cu}^I$ , $\text{Cu}^{1.5}\text{Cu}^{1.5}$ , and $\text{Cu}^{II}\text{Cu}^{II}$

Neal P. Mankad, Eric Rivard, Seth B. Harkins, and Jonas C. Peters\*

Division of Chemistry and Chemical Engineering, Arnold and Mabel Beckman Laboratories of Chemical Synthesis, California Institute of Technology, Pasadena, California 91125

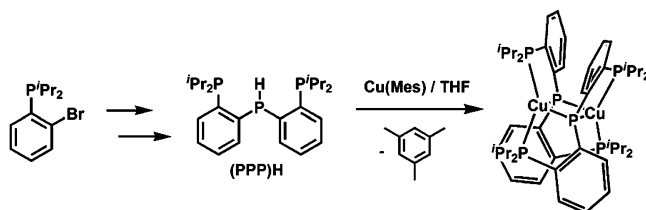
Received September 2, 2005; E-mail: jpeters@caltech.edu

Understanding how nature controls electron transfer (ET) rates in copper-containing proteins, such as the “blue copper” protein family, has provided impetus for theoretical, biochemical, and small molecule model studies.<sup>1</sup> It is generally accepted that structural reorganization as a function of ET needs to be minimized if rapid rates are to be achieved,<sup>2</sup> and that this can be difficult to accomplish in synthetic copper systems due to ligand rearrangement, loss, and exchange processes.<sup>3</sup> Recently, we described an amido-bridged  $\text{Cu}_2\text{N}_2$  system,  $\{(\text{SNS})\text{Cu}\}_2$  (**1**) ( $[\text{SNS}]^-$  = bis(2-*tert*-butylsulfanylphenyl)amide),<sup>4</sup> that shares the diamond core structural motif of the  $\text{Cu}_A$  site<sup>5</sup> and reversibly accommodates rapid ET via low overall structural reorganization.<sup>6</sup> Because the copper centers in **1** possess geometries intermediate between tetrahedral and square planar (coined *pseudotetrahedral* herein), we thought ligand modification might provide reversible access to a third, formally  $\text{Cu}^{II}\text{Cu}^{II}$  species. Furthermore, we have described a highly luminescent  $\text{Cu}_2\text{N}_2$  system,  $\{(\text{PNP})\text{Cu}\}_2$  (**2**) ( $[\text{PNP}]^-$  = bis(2-*di-iso*-butylphosphinophenyl)amide), that mediated two fully reversible redox events according to CV data.<sup>7,8</sup> We thus sought to replace the amide bridging ligands in **2** with more electron-releasing phosphides to further stabilize the doubly oxidized species and to afford us the possibility of isolating and structurally analyzing the system across the oxidation states  $\text{Cu}^I\text{Cu}^I$ ,  $\text{Cu}^{1.5}\text{Cu}^{1.5}$ , and  $\text{Cu}^{II}\text{Cu}^{II}$ .

Here we describe the characterization of a phosphido-bridged dicopper system,  $\{(\text{PPP})\text{Cu}\}_2$  (**3**) ( $[\text{PPP}]^-$  = bis(2-*di-iso*-propylphosphinophenyl)phosphide), in which each Cu center maintains a highly distorted tetrahedral geometry across these three oxidation states. While the overall topology of each structure is very similar to those  $\text{Cu}_2\text{N}_2$  systems we have described previously, the  $\text{Cu}_2\text{P}_2$  system displays remarkable flexibility at the phosphide hinge to allow for dramatic changes in both the  $\text{Cu}\cdots\text{Cu}$  distance and the  $\text{Cu}-\text{P}_\mu-\text{Cu}$  angle as a function of oxidation state. Dicopper systems that can reversibly access three discrete oxidation states were essentially unknown prior to this study. Indeed, a complete set of structural data for any such transition metal system is rare. Most relevant to the current study is an aryloxide-bridged  $\text{Fe}_2\text{O}_2$  system that was structurally characterized in the oxidation states  $\text{Fe}^{II}\text{Fe}^{II}$ ,  $\text{Fe}^{II}\text{Fe}^{III}$ ,  $\text{Fe}^{III}\text{Fe}^{III}$ .<sup>9</sup> The structural analyses of systems supported by redox-active ligands across three oxidation states have also been described.<sup>10</sup>

To prepare the dicopper system of interest to us (Scheme 1), a chlorophosphine precursor of (PPP)H was synthesized by *ortho*-lithiation of 2-*di-iso*-propylphosphinophenyl bromide with *n*-butyllithium, followed by addition of 0.5 equiv of  $\text{PCl}_3$ . Subsequent reduction of the resulting diarylchlorophosphine by  $\text{LiAlH}_4$  gave (PPP)H as a colorless oil. The reaction of (PPP)H with mesitylcopper(I) gave diamagnetic red–orange **3** ( $^{31}\text{P}$  NMR (ppm): 34.0 (br, 4P), –21.0 (br, 2P)) with concomitant formation of mesitylene. XRD analysis of suitable crystals of **3** confirmed its dimeric diamond-core structure (Figure 1). The most striking difference between the structure of **3** and previously characterized  $\text{Cu}_2\text{N}_2$

Scheme 1



systems<sup>4,7</sup> is its much longer  $\text{Cu}\cdots\text{Cu}$  distance (3.307(2) Å for **3** vs 2.5989(3) Å for **1** and 2.6245(8) Å for **2**) resulting from the larger phosphide bridging groups. The  $\text{Cu}-\text{X}-\text{Cu}$  angles are likewise expanded ( $\text{Cu}-\text{P}_\mu-\text{Cu}$  (avg) =  $90.63^\circ$  for **3** vs  $\text{Cu}-\text{N}-\text{Cu}$  (avg) =  $75.72^\circ$  for **1** and  $74.07^\circ$  for **2**).

Figure 2a compares the cyclic voltammetry of **3** and its  $\text{Cu}_2\text{N}_2$  relative **2**. Two fully reversible redox events are observed for each system. There is a large cathodic shift of approximately 600 mV for each redox couple of the phosphide-bridged system **3**. Its

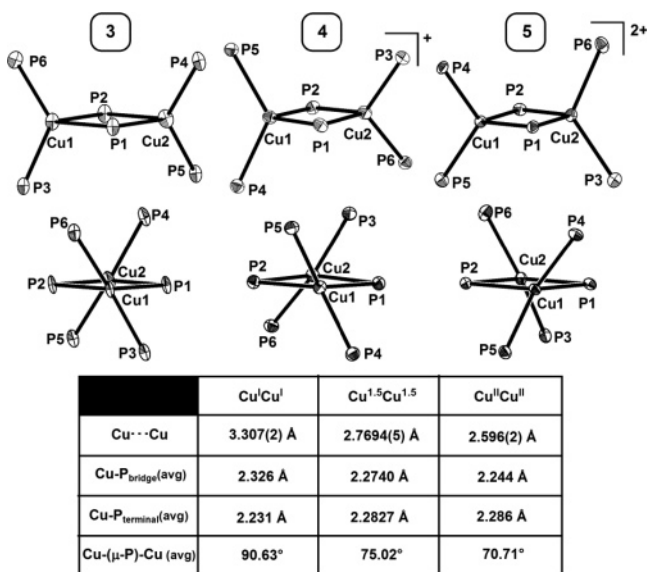


Figure 1. Pertinent X-ray data for complexes **3**, **4**, and **5**.

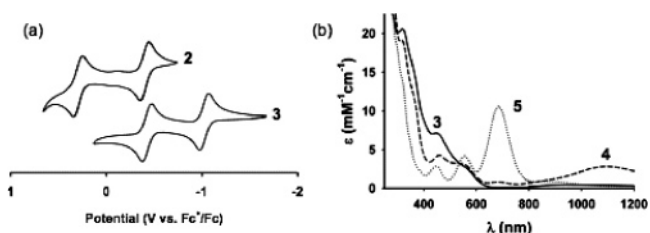


Figure 2. (a) Cyclic voltammograms of **2** and **3** (THF, 0.35 M [ $^n\text{Bu}_4\text{N}$ ][ $\text{PF}_6$ ], 200 mV/s) vs  $\text{Fc}^+/\text{Fc}$ . (b) Optical spectra for **3** (solid), **4** (dashed), and **5** (dotted).

$\text{Cu}^{1.5}\text{Cu}^{1.5}/\text{Cu}^{\text{I}}\text{Cu}^{\text{I}}$  couple is assigned at  $E^{\circ} = -1.02$  V, and its  $\text{Cu}^{\text{II}}\text{Cu}^{\text{II}}/\text{Cu}^{1.5}\text{Cu}^{1.5}$  couple is assigned at  $E^{\circ} = -0.42$  V.

Chemical oxidation of **3** with 1 equiv of  $[\text{FeCp}_2][\text{BPh}_4]$  yielded the red–purple paramagnetic species  $[\{(\text{PPP})\text{Cu}\}_2][\text{BPh}_4]$  (**4**). The X-band EPR spectrum of **4** at 10 K showed an isotropic  $S = 1/2$  signal. The complex hyperfine splitting pattern features components from the two Cu centers and the phosphide bridges (see Supporting Information). These data, along with a signature low-energy intervalence charge-transfer band at 1095 nm ( $\epsilon = 2800 \text{ M}^{-1} \text{ cm}^{-1}$ , Figure 2b), suggest that **4** be described as a delocalized mixed-valence system.<sup>11</sup>

This electronic structure for **4** was at first surprising to us given the unusually long  $\text{Cu}\cdots\text{Cu}$  distance present in **3**, but XRD analysis revealed that one-electron oxidation of **3** also resulted in a huge  $\text{Cu}-\text{Cu}$  contraction ( $\text{Cu}\cdots\text{Cu} = 2.7694(5) \text{ \AA}$  in **4**, see Figure 1). This 0.538 Å contraction is accompanied by a dramatic compression of the average  $\text{Cu}-\text{P}_\mu-\text{Cu}$  angle from 90.63° in **3** to 75.02° in **4**. While modest distortions of a similar nature are observed upon one-electron oxidation of **1**,<sup>4</sup> the  $\text{Cu}_2\text{P}_2$  system is unexpectedly flexible. Despite the structural compression that occurs upon oxidation, there is complete retention of the pseudotetrahedral Cu centers and the dimeric topology.

Two-electron oxidation of **3** with 2 equiv of  $[\text{FeCp}_2][\text{BAr}^{\text{F}}_4]$  ( $\text{Ar}^{\text{F}} = 3,5\text{-(CF}_3)_2\text{C}_6\text{H}_3$ ) yielded  $[\{(\text{PPP})\text{Cu}\}_2][\text{BAr}^{\text{F}}_4]_2$  (**5**), a deep blue–purple compound with an intense LMCT absorption at 683 nm ( $\epsilon = 10\,600 \text{ M}^{-1} \text{ cm}^{-1}$ , Figure 2b).  $^1\text{H}$ ,  $^{13}\text{C}$ ,  $^{19}\text{F}$ , and  $^{31}\text{P}$  NMR resonances were observed for **5**, consistent with population of an  $S = 0$  ground state at room temperature.  $^{31}\text{P}\{^1\text{H}\}$  NMR resonances occur at 266.1 (2P) and 37.3 ppm (4P) in  $\text{CD}_2\text{Cl}_2$ . The extreme downfield chemical shift of the bridging phosphide resonance of **5** is likely the result of the large change in bond angles at the bridging phosphides.<sup>12,13</sup>

Though suitable single crystals of **5** proved elusive, using  $\text{AgSbF}_6$  instead of  $[\text{FeCp}_2][\text{BAr}^{\text{F}}_4]$  afforded the more readily crystallized salt  $[\{(\text{PPP})\text{Cu}\}_2][\text{SbF}_6]_2$ . Its molecular structure reveals two  $\text{SbF}_6$  anions per dimeric unit, and it is gratifying to observe that the  $\text{Cu}_2\text{P}_2$  diamond core is maintained along with retention of pseudotetrahedral geometries at each copper center (Figure 1). Close examination of the bond parameters reveals a further contraction of the  $\text{Cu}\cdots\text{Cu}$  distance (2.596(2) Å) and further compression of the average  $\text{Cu}-\text{P}_\mu-\text{Cu}$  angle (70.71°). Although the onset of a direct bonding interaction between the two 17-electron centers upon oxidation cannot be dismissed, it is plausible that the  $\text{Cu}\cdots\text{Cu}$  contraction is a consequence of an optimized bridging angle that facilitates exchange coupling between the Cu centers.<sup>14</sup> Indeed, the simplest oxidation state description for **5** involves two strongly antiferromagnetically coupled  $\text{Cu}^{\text{II}}$  centers. The prototypical  $\text{Cu}_2\text{Cl}_6^{2-}$  dianion, whose structure is very similar to that of **5**, also features two  $\text{Cu}^{\text{II}}$  centers that are either ferromagnetically or antiferromagnetically coupled depending on the choice of counterion and the resulting perturbations in bond angles.<sup>14c</sup> The structure of **5** is distinctive because small-molecule  $\text{Cu}^{\text{II}}$  ions residing in pseudotetrahedral coordination environments are rare.<sup>15</sup> Moreover, few examples of  $\text{Cu}^{\text{II}}$  phosphine complexes are known,<sup>16</sup> and only one previous example has been structurally characterized.<sup>16a</sup>

A ramification of the elasticity of the  $\text{Cu}_2\text{P}_2$  core manifests itself in the luminescence behavior of **3**. Excitation into the low-energy absorptions of **3** ( $\lambda_{\text{ex}} = 500 \text{ nm}$ ) afforded an emission spectrum with  $\lambda_{\text{max}} = 687 \text{ nm}$ . This emission band is much broader and quite red-shifted compared to that of the amide derivative **2**.<sup>7</sup> The reorganizational energy upon excitation, which can be estimated using the width of an emission band,<sup>17</sup> is accordingly higher for **3** (ca.  $3250 \text{ cm}^{-1}$ ) relative to **2** (ca.  $2600 \text{ cm}^{-1}$ ). In addition, while **2**

is known to have an extremely high quantum yield ( $\phi = 0.67(4)$ ) and a long excited-state lifetime ( $\tau = 10.9(4) \mu\text{s}$ ) in THF at 298 K,<sup>7</sup> corresponding emission measurements for **3** reveal significantly lower values ( $\phi = 0.013(3)$  and  $\tau = 0.6(3) \mu\text{s}$ ). It seems most likely that this attenuation in emission is related to a greater degree of structural reorganization upon MLCT in **3** than in **2**.

To summarize, we have shown that synthetic dicopper centers bridged in the diamond-core structural motif become unusually redox active, in this case sampling the oxidation states  $\text{Cu}^{\text{I}}\text{Cu}^{\text{I}}$ ,  $\text{Cu}^{1.5}\text{Cu}^{1.5}$ , and  $\text{Cu}^{\text{II}}\text{Cu}^{\text{II}}$ . The auxiliary ligand preserves a geometry that is midway between square planar and tetrahedral about each copper center, yet is flexible enough to accommodate pronounced changes in the  $\text{Cu}\cdots\text{Cu}$  distance as a function of ET.

**Acknowledgment.** We thank the BP MC<sup>2</sup> program for financial support. N.P.M. was supported by an NSF graduate research fellowship, and E.R. by an NSERC postdoctoral fellowship. Larry Henling, Ted Betley, Brian Leigh, and Dr. Angelo Di Bilio provided technical assistance. The Zewail group provided access to a near-IR spectrometer. Luminescence measurements were acquired at the Beckman Institute Laser Resource Center.

**Supporting Information Available:** Experimental and characterization data; crystallographic data. This material is available free of charge via the Internet at <http://pubs.acs.org>.

## References

- (1) (a) Gray, H. B.; Malmstrom, B. G.; Williams, R. J. P. *J. Biol. Inorg. Chem.* **2000**, *5*, 551. (b) Rorabacher, D. B. *Chem. Rev.* **2004**, *104*, 651.
- (2) Marcus, R. A.; Sutin, N. *Biochim. Biophys. Acta* **1985**, *811*, 265.
- (3) Azacryptand ligands can overcome the need for large structural reorganization and ligand addition/loss/exchange. See: Nelson J.; McKee, V.; Morgan, G. G. *Prog. Inorg. Chem.* **1998**, *47*, 167.
- (4) Harkins, S. B.; Peters, J. C. *J. Am. Chem. Soc.* **2004**, *126*, 2885.
- (5) (a) Williams, P. A.; Blackburn, N. J.; Sanders, D.; Bellamy, H.; Stura, E. A.; Fee, J. A.; McRee, D. E. *Nat. Struct. Biol.* **1999**, *6*, 509. (b) DeBeer George, S.; Metz, M.; Szilagyi, R. K.; Wang, H.; Cramer, S. P.; Lu, Y.; Tolman, W. B.; Hedman, B.; Hodgson, K. O.; Solomon, E. I. *J. Am. Chem. Soc.* **2001**, *123*, 5757. (c) Gamelin, D. R.; Randall, D. W.; Hay, M. T.; Houser, R. P.; Mulder, T. C.; Canters, G. W.; de Vries, S.; Tolman, W. B.; Lu, Y.; Solomon, E. I. *J. Am. Chem. Soc.* **1998**, *120*, 5246.
- (6) For other examples of dicopper class III mixed-valence species, see: (a) Houser, R. P.; Young, V. G., Jr.; Tolman, W. B. *J. Am. Chem. Soc.* **1996**, *118*, 2101. (b) He, C.; Lippard, S. J. *Inorg. Chem.* **2000**, *39*, 5225.
- (7) Harkins, S. B.; Peters, J. C. *J. Am. Chem. Soc.* **2005**, *127*, 2030. Our efforts to further characterize this  $\text{Cu}_2\text{N}_2$  system will be reported in due course.
- (8) A dicopper system has been recently described for which CV data indicate two pseudo-reversible redox events. Uptake of an additional ligand occurs upon oxidation of the  $\text{Cu}^{\text{I}}\text{Cu}^{\text{I}}$  to the  $\text{Cu}^{1.5}\text{Cu}^{1.5}$  state: Jiang, X.; Bollinger, J. C.; Baik, M.-H.; Lee, D. *Chem. Commun.* **2005**, 1043.
- (9) Snyder, B. S.; Patterson, G. S.; Abrahamson, A. J.; Holm, R. H. *J. Am. Chem. Soc.* **1989**, *111*, 5214.
- (10) For example: (a) Sellmann, D.; Binder, H.; Häussinger, D.; Heinemann, F. W.; Sutter, J. *Inorg. Chim. Acta* **2000**, *300–302*, 829. (b) Huynh, M. H. V.; El-Samanody, E.-S.; White, P. S.; Meyer, T. J. *Inorg. Chem.* **1999**, *38*, 3760.
- (11) Robin, M.; Day, P. *Adv. Inorg. Radiochem.* **1967**, *10*, 247.
- (12) For discussions on bridging phosphide  $^{31}\text{P}$  NMR resonances relating to metal–metal bonding, see: (a) Targos, T. S.; Geoffroy, G. L.; Rheingold, A. L. *Organometallics* **1986**, *5*, 12 and references therein. (b) Cartwright, S. J.; Dixon, K. R.; Rattray, A. D. *Inorg. Chem.* **1980**, *19*, 1120.
- (13) For a discussion on the dependence of  $^{31}\text{P}$  chemical shifts on bond angle, see: Garrou, P. E. *Chem. Rev.* **1981**, *81*, 229.
- (14) For discussions on the effect of bridging angle on coupling between  $d^9$  centers in dicopper systems, see: (a) Charlot, M. F.; Jeannin, S.; Jeannin, Y.; Kahn, O.; Lucrece-Abaul, J.; Martin-Frere, J. *Inorg. Chem.* **1979**, *18*, 1675. (b) Crawford, V. H.; Richardson, H. W.; Wasson, J. R.; Hodgson, D. J.; Hatfield, W. E. *Inorg. Chem.* **1976**, *15*, 2107. (c) Hay, P. J.; Thibault, J. C.; Hoffmann, R. *J. Am. Chem. Soc.* **1975**, *97*, 4884.
- (15) For examples, see: (a) Baumann, F.; Livoreil, A.; Kaim, W.; Sauvage, J.-P. *Chem. Commun.* **1997**, 35. (b) Tolman, W. B. *Inorg. Chem.* **1991**, *30*, 4877. (c) Knapp, S.; Keenan, T. P.; Zhang, X.; Fikar, R.; Potenza, J. A.; Schugar, H. J. *J. Am. Chem. Soc.* **1990**, *112*, 3452. (c) Kitajima, J.; Fujisawa, K.; Moro-oka, Y. *J. Am. Chem. Soc.* **1990**, *112*, 3210 and references therein.
- (16) (a) Pilloni, G.; Bandoli, G.; Tisato, F.; Corain, B. *Chem. Commun.* **1996**, 433. (b) Lobana, T. S.; Bhatia, P. K. *J. Chem. Soc., Dalton Trans.* **1992**, 1407. (c) Zelonka, R. A.; Baird, M. C. *Chem. Commun.* **1971**, 780.
- (17) See Supporting Information for details.

JA056071L